Published as: *Nat Neurosci*. 2005 February ; 8(2): 149–155.

Ca^{2+} current - driven nonlinear amplification by the mammalian cochlea *in vitro*

Dylan K. Chan and **A. J. Hudspeth**
Laboratory of Sensory Neuroscience and Howard Hughes Medical Institute, The Rockefeller University, 1230 York Avenue, New York, New York 10021, USA.

Abstract

An active process in the inner ear expends energy to enhance the sensitivity and frequency selectivity of hearing. Two mechanisms have been proposed to underlie this process in the mammalian cochlea: receptor-potential-based electromotility and Ca^{2+}-driven active hair-bundle motility. To link the phenomenology of the cochlear amplifier with these cellular mechanisms, we developed an *in vitro* cochlear preparation from *Meriones unguiculatus* that affords optical access to the sensory epithelium while mimicking its *in vivo* environment. Acoustic and electrical stimulation elicited microphonic potentials and electrically evoked hair-bundle movement, demonstrating intact forward and reverse mechanotransduction. The mechanical responses of hair bundles from inner hair cells revealed a characteristic resonance and a compressive nonlinearity diagnostic of the active process. Blocking transduction with amiloride abolished nonlinear amplification, whereas eliminating all but the Ca^{2+} component of the transduction current did not. The results suggest that the Ca^{2+} current drives the cochlear active process and support the hypothesis that active hair-bundle motility underlies cochlear amplification.

INTRODUCTION

The active process that optimizes the inner ear's response to sound is defined by four principal characteristics[1–6]. First, the active process expends energy to amplify sound stimuli. Second, its activity is frequency-specific, thus greatly sharpening the acoustic response. Third, the active process displays a compressive nonlinearity that condenses a wide range of stimulus intensities into a narrow gamut of responses. Finally, it underlies the production of sound by the ear, a phenomenon termed spontaneous otoacoustic emission. Present in all tetrapod vertebrates, the active process accounts for the ear's exquisite sensitivity and acuity, as well as for its prodigious range of responsiveness in terms of frequency and intensity.

In the mammalian cochlea, the active process resides in the outer hair cells of the organ of Corti, which sits atop an elastic basilar membrane whose vibration is maximally sensitive to a range of characteristic frequencies ordered tonotopically along its length[2]. Several specializations of the cochlea are critical for the operation of the active process. The micromechanical arrangement of cells within the organ of Corti is essential for sound, in the form of pressure differences across the basilar membrane, to stimulate the hair cells. In addition, the fluid environment of the cochlea is unique: the mechanosensitive hair bundles on the apical surface of the sensory epithelium are bathed in endolymph, a K^+-rich and Na^+-poor solution containing only ~25 μM of Ca^{2+}, whereas the basolateral cellular surfaces are exposed to perilymph, which is similar to extracellular fluid in composition. Disruption of this specialized environment causes significant structural changes, especially to the tectorial membrane[7], and leads to cellular intoxication with inappropriate ions. Finally, there is normally a standing

Correspondence should be addressed to A. J. H. (hudspaj@rockefeller.edu).

endocochlear potential across the epithelium such that the apical compartment is ~80 mV positive relative to the basolateral compartment; the active process falters in the absence of this potential[8,9]. *In vivo* laser interferometry of basilar-membrane movement, which preserves these specializations, has permitted extensive characterization of the macroscopic phenomenology of the cochlear amplifier[2–6]. Because disruption of the cochlear microenvironment upon acute dissection has precluded the investigation of nonlinear amplification *in vitro*[10,11], however, the cellular basis of the active process is poorly understood.

Two mechanisms have been proposed to underlie the cochlear active process in mammals. The first, somatic electromotility, is effected by prestin, a protein abundant in the plasma membrane of the outer hair cell[12–14]. In response to changes in the membrane potential, prestin alters its conformation and, in consequence, the length of the cell itself. Prestin is required for normal hearing: knockout of the cognate gene yields mice with severely attenuated responses to sound[15]. The second candidate mechanism, active hair-bundle motility, is based on the bundle's capacity to exert forces that amplify mechanical stimuli[16–19]. In this case, force arises from the myosin motors involved in adaptation[20] and from the Ca^{2+}-dependent reclosure of transduction channels[21,22], both of which are driven by the Ca^{2+} current entering the hair cell as a consequence of mechanoelectrical transduction. Active hair-bundle motility has been shown to produce all of the characteristics of the active process in non-mammalian tetrapods[1], but its significance in mammals remains unknown.

In this paper, we describe an *in vitro* preparation of the cochlea from *Meriones unguiculatus*, the clawed jird or Mongolian "gerbil," that permits observation of cochlear amplification and evaluation of the competing hypotheses concerning its origin. We find that Ca^{2+} flow through the mechanoelectrical-transduction channel is both necessary and sufficient for nonlinear amplification, suggesting an important role for active hair-bundle motility in the cochlear active process.

RESULTS

In vitro preparation of the mammalian cochlea

To study cochlear amplification *in vitro*, we developed an experimental preparation that recapitulates the *in vivo* properties of the cochlea while providing optical and electrical access to the hair cells themselves. By mounting the excised middle turn of the cochlea in a two-compartment recording chamber that allows the delivery of acoustic stimuli, we isolated the apical and basal aspects of the sensory epithelium and bathed them in readily exchangeable K^+-rich endolymph and Na^+-based perilymph solutions, respectively (Fig. 1a,b). Both visual observation and the measured transepithelial resistance of ~2 kΩ confirmed the absence of significant leakage between the two compartments. The tectorial membrane remained in place and extended beyond the third row of outer hair cells. Because the preparation generally began to show signs of morphological and physiological deterioration 30–60 min after dissection, we performed all of our experiments within 30 min. During this time, the preparation was judged to be viable by two criteria. First, both the inner and outer hair cells appeared healthy upon microscopic inspection, without swelling, bundle malformations, or brownian motion of organelles (Fig. 1c–e). Second, as described below, the preparation displayed electrical and mechanical responses to stimulation.

During stimulation with sound of a particular frequency, the pressure gradient across the basilar membrane sets this elastic structure into oscillation. Basilar-membrane movement is communicated to the overlying organ of Corti, where shearing movements of the tectorial membrane deflect the hair bundles of inner hair cells, the ultimate acoustic detectors of the inner ear. The tectorial membrane also stimulates outer hair cells, which implement the active

process by increasing the amplitude of basilar-membrane oscillation through the mechanism under investigation. To keep the experimental preparation as intact as possible, we did not disturb the tight mechanical and hydrodynamic coupling among the basilar membrane, organ of Corti, and tectorial membrane. Instead, we used the mechanical responses of inner hair cells —whose hair bundles produce microscopic images with sharp contrast—to investigate the nature of the active process in outer hair cells (Fig. 1d).

Acoustic properties

Acoustic stimuli were provided through the lower compartment to the basal aspect of the sensory epithelium. To determine the acoustic properties of the system, we sealed a pressure transducer onto the recording chamber in place of the cochlear preparation and recorded the pressure in response to acoustic frequency sweeps. We detected slight fluctuations in the pressure amplitude with frequency; calibration of the earphone's output against these irregularities eliminated the fluctuations, thus permitting the delivery to the sensory epithelium of a known pressure stimulus that was flat across the frequency range of 0.3–3.0 kHz (Fig. 2a,b).

When an acoustic frequency sweep was applied, hair-bundle movements exhibited a striking resonance (Fig. 2a) that was fit well by the Lorentzian relation characteristic of a second-order harmonic oscillator (Fig. 2c). As the resonance was traversed, the displacement response acquired a phase lag of π radians relative to the pressure stimulus. The phase of movement was constant throughout the exposed cochlear segment, indicating that the experimental conditions suppressed the traveling wave that traverses the basilar membrane *in vivo*. In a dead and thus passive preparation, the peak's magnitude scaled linearly with stimulus intensity over a range of 60 dB (Fig. 2d). The resonant frequency was insensitive to the volume of liquid in the upper compartment but highly dependent upon that in the lower, in which 2–5 μl of perilymph yielded resonant frequencies of 400–1100 Hz, comparable to the range of 700–1500 Hz expected for this cochlear segment[23]. The frequency scaled inversely with the square root of the lower liquid mass, allowing us to calculate the stiffness of the isolated segment of basilar membrane as ~120 $N \cdot m^{-1}$. This value increased by ~65% after formaldehyde fixation and by ~200% after exposure to glutaraldehyde, confirming that the basilar membrane dominated the system's stiffness (Fig. 2e).

Microphonic potential

A basic metric for the health of a hair cell is its ability to conduct mechanoelectrical transduction. To test the integrity of this mechanism, we measured its extracellular manifestation, the microphonic potential. In response to 60–80 dB stimuli at the resonant frequency of each preparation, we recorded microphonic potentials 10–50 μV in peak-to-peak magnitude. Simultaneous recording of the microphonic potential and vertical velocity of the tectorial membrane revealed that the phase of positive polarization of the lower compartment, which correlates with current flowing into hair cells, lagged the velocity towards scala media by $\pi/2$ (Fig. 3a); this accords with the conventional model of cochlear mechanics in which displacement towards scala media causes mechanoelectrical-transduction channels to open[10,24]. Consistent with its origin in the hair cells, the microphonic potential displayed a resonance at a frequency that matched that of the mechanical responses and saturated at high stimulus intensities.

The microphonic potential was reversibly abolished by filling the upper compartment with endolymph containing amiloride (Fig. 3b). A concentration-response curve revealed a half-maximal inhibitory concentration (K_I) of 96 μM (Fig. 3e), indicating that the inhibitory activity of amiloride results from its blockage of the mechanoelectrical-transduction channel, and not of other receptors[25]. Application of 50 μM streptomycin, a structurally dissimilar transduction-

channel blocker, also abolished the microphonic response (data not shown), as did treatment with endolymph in which K^+ was replaced as the primary monovalent cation by *N*-methyl-**D**-glucamine (NMDG), which does not traverse the transduction channel[26] (Fig. 3c). Application of a transepithelial potential to mimic the *in vivo* endocochlear potential changed the driving force on ions entering the hair cell and accordingly had a strong effect on the microphonic potential (Fig. 3d). The saturation observed at high and low transepithelial potentials may reflect the activation of voltage-dependent conductances at these extreme extracellular potentials and of adaptation in the transduction machinery. The reversal of response polarity at a transepithelial potential near −50 mV indicates that the resting potentials of the hair cells were near that value, demonstrating their electrical integrity. Taken together, these results show that the hair cells could be stimulated effectively and functioned normally *in vitro*.

Electrically evoked hair-bundle movement

Each of the proposed mechanisms for the cochlear active process involves some form of reverse electromechanical transduction. To detect such a transduction process, we applied electrical stimuli across the sensory epithelium and monitored hair-bundle displacement. Application of 5–40-μA stimuli in the form of 500-Hz sinusoids or 50-ms pulses elicited bundle movements up to 40 nm in peak-to-peak magnitude. These responses were abolished reversibly by amiloride with a K_I of 75 μM, confirming their dependence upon mechanoelectrical transduction (Fig. 4a). Small transients remained at the beginning and end of the response to the electrical pulse even in the presence of amiloride. Because these transients could not be abolished by treatment with BAPTA, which disrupts tip links[27], or salicylate, a blocker of electromotility[28], they likely represent stimulation artifacts that underlie the residual signal in the sinusoidal response as well. The electrical responses of hair bundles were not affected by substitution of NMDG-based endolymph, which lacks the K^+ that ordinarily carries most of the transduction current (Fig. 4b)[29]. This result implies that the entry of Ca^{2+}, which persists in NMDG endolymph, is sufficient to mediate the full extent of electrically evoked hair-bundle movement.

Nonlinear amplification

The selective amplification of low-intensity stimuli by the cochlear amplifier is manifested in the compressive nonlinearity of the basilar membrane's response to pressure stimuli[2]. To seek this nonlinearity *in vitro*, we measured the displacement of hair bundles in response to acoustic frequency sweeps over a ~50-dB range of stimulus intensities. In the presence of normal, K^+-based endolymph and an applied transepithelial potential of +80 mV, we observed a compressive nonlinearity in the stimulus-response function (Fig. 5a), especially at low levels of stimulation. In a doubly logarithmic plot of hair-bundle displacement as a function of sound pressure, the slope over the 30–60-dB range was 0.74 (r^2 = 0.94); this value differs significantly from that of unity corresponding to linear responsiveness. When the transepithelial potential was absent or amiloride was applied, the response became linear, with slopes of 1.06 (r^2 = 0.99) and 1.17 (r^2 = 0.99), respectively (Fig. 5a). By contrast, the compressive nonlinearity persisted with a slope of 0.74 (r^2 = 0.99) in the presence of NMDG-based endolymph and a +80-mV transepithelial potential (Fig. 5b). Under these conditions, the sensitivity of hair-bundle displacement was greatest at the lowest stimulus intensity (Fig. 5c). These results indicate that the Ca^{2+} component of the transduction current, and not the dominant K^+ component, is necessary and sufficient to drive the active process that underlies cochlear amplification. Because Ca^{2+} is required to maintain the integrity of tip links[27], however, it was not possible to test the consequences of the ion's complete removal on amplification.

To compare more directly the nonlinearity observed here with that traditionally measured *in vivo*, we used laser interferometry to measure the vertical motion of a bead placed atop the tectorial membrane above an inner hair cell. In the presence of a +80-mV transepithelial

potential and NMDG-based endolymph, a compressive nonlinearity with a slope of 0.85 (r^2 = 1.00) was observed in the response to stimuli at the resonant frequency (Fig. 5d). In the absence of the transepithelial potential, the response was linear, with a power-law slope of 1.07 (r^2 = 0.99).

Although it was difficult to compare the absolute magnitudes of responses across experiments, the power-law dependences of bundle displacement on sound pressure were highly consistent. In the presence of K^+-rich control endolymph, the mean slope in the 30–60-dB range of stimulus intensities was 0.81 ± 0.12 (n = 15). Substitution of NMDG for K^+ yielded a slope of 0.74 ± 0.15 (n = 16), which is not significantly different ($P > 0.14$). By contrast, K^+ endolymph containing amiloride yielded a slope of 1.04 ± 0.14 (n = 17), which differs significantly from each of the other two values ($P < 0.001$). These nonlinearities reveal an amiloride-sensitive active amplifier that operates in the presence of either K^+- or NMDG-based endolymph.

Adjustment of the transepithelial potential provided a rapid and reversible means of altering the effectiveness of the active process without physically perturbing the preparation. When this potential was reduced from +80 mV to 0 mV, the response immediately diminished; reapplying the positive potential restored the original response. We compared the bundle displacement at the resonant peak in the presence of a +80-mV transepithelial potential to the displacements obtained immediately before and after in the absence of the applied potential. In the presence of K^+ endolymph, this ratio was 1.33 ± 0.53 (n = 23); substitution with NMDG endolymph yielded a ratio of 1.22 ± 0.37 (n = 54), which is not significantly different ($P > 0.19$). In contrast, this ratio in the presence of amiloride was 0.97 ± 0.10 (n = 27), which differs significantly from the values obtained in K^+ endolymph ($P < 0.003$) and NMDG endolymph ($P < 0.00003$). The ~1.3-fold amplification observed when K^+ or NMDG endolymph, but not amiloride, bathed the apical surface corroborates the results of the nonlinear slope analysis.

DISCUSSION

An active *in vitro* preparation of the mammalian cochlea

The operation of cochlear hair cells is inextricably linked with their ionic, electrical, and mechanical environment. Any study of these cells' functions—especially one meant to address their role in the cochlear active process—is limited by the extent to which this *in vivo* environment can be mimicked. By separating the ionic environments of the epithelium's apical and basal surfaces, maintaining a transepithelial current that reproduces the *in vivo* endocochlear potential, and providing acoustic stimuli that drive basilar-membrane movement with pressure gradients, we were able to observe active responses from the organ of Corti *in vitro*.

Although we measured the radial displacement of hair bundles in this study, most previous investigations have instead tracked the vertical displacement of the basilar membrane. Modeling suggests, however, that the structure of the cochlear partition imposes an approximately unity gain between basilar-membrane movement and hair-bundle displacement[30], and our preliminary laser-interferometric measurements of basilar-membrane displacement in the present preparation support this notion (data not shown). Taking this into account, the resonant frequency, Q_0, peak sensitivity, and basilar-membrane stiffness determined here are all comparable to those obtained *in vivo*[2,5,6,20,31]. It is therefore likely that the cochlear partition in this preparation responds to sound much as it does in the intact ear. Furthermore, the presence of a microphonic potential sensitive to transduction-channel blockade and transepithelial potential, as well as a mechanical response to electrical stimuli, attests to the health of the hair cells and integrity of both forward and reverse mechanoelectrical transduction. Finally, the hair bundle's response to sound pressure displayed a compressive nonlinearity and was sensitive to the transepithelial potential, instantiating the cochlear active

process in this preparation. This nonlinearity was comparable in both the radial component of hair-bundle response and in the vertical component of cochlear-partition motion, suggesting linear coupling between these two motions and permitting comparison between the present nonlinearity and those studied in the past *in vivo*.

The nonlinearity observed here differs somewhat from that described for the cochlear base[2]. Although the response became linear at high levels of stimulation, as it does when measured *in vivo*, the limited sensitivity of our recording technique precluded observation of the complementary linearization at very low stimulus levels[4]. Within the nonlinear range, the power-law slope of 0.7–0.8 does not reach the value of 0.3–0.4 observed at the cochlear base[5,6]. This difference may be temperature-related: the recording location was maintained by the illumination system at 31°, a value below the optimal operating temperature of the amplifier[32]. Moreover, any mismatch between the experimental system's resonant frequency and the natural frequency of the cochlear segment might have lowered the power-law exponent. Finally, the difference may reflect a diminution in amplification towards the cochlear apex, as has been noted in studies of both basilar-membrane motion and auditory-nerve activity[33,34]. Such a gradient may also explain the relatively poor frequency selectivity of the nonlinearity seen in this preparation and at the cochlear apex[33]; this broad tuning may actually serve to minimize the effects of the resonance mismatch[35]. If this gradient were physiologically relevant, our *in vitro* nonlinearity, like the passive mechanical characteristics described above, would fall well within the range expected for this cochlear turn as predicted by interpolation of observations made at the cochlear base and apex[2].

A Ca^{2+} current-based mechanism for cochlear amplification

Application of amiloride or removal of the transepithelial potential, by respectively blocking mechanoelectrical-transduction channels or reducing the driving force on permeant ions, severely attenuated the microphonic potential and linearized the bundle's response to acoustic stimuli. This finding provides strong evidence that the cochlear amplification observed here rests upon the mechanoelectrical-transduction apparatus rather than a transduction-independent mechanism[36]. On the other hand, when the apical surface of the sensory epithelium was bathed in NMDG-based endolymph and a transepithelial potential was applied, little microphonic potential could be recorded, yet amplification was still observed. This dissociation of the receptor potential, as reflected in the microphonic potential, from the active process, as revealed by the compressive nonlinearity, argues against the participation of any membrane-potential-based process such as somatic electromotility at the frequencies studied here. The possibility remains, however, that electromotility plays a role in higher-frequency amplification at the cochlear base.

In the presence of NMDG-based endolymph, only the small transduction current carried by the 25 μM Ca^{2+} and 1 mM Na^{+} in the apical solution entered the hair cells. This current would not generate a substantial receptor potential, and thus could not support large-scale conformational changes in prestin. It has been demonstrated, however, that Ca^{2+} current alone is sufficient to drive active hair-bundle motility: a solution similar to the NMDG-based endolymph used here, in which the only transduction channel-permeant ions present were small amounts of Ca^{2+} and Na^{+}, nonetheless supported spontaneous hair-bundle movement and active amplification by the hair cells of the bullfrog's sacculus[16]. A similar Ca^{2+}-current-based mechanism likely underlies the nonlinearity and amplification observed in this study.

Correlates of the two mechanisms for active hair-bundle motility in non-mammalian tetrapods, a slow one based on myosin motors and a fast one based on Ca^{2+}-dependent channel reclosure, have been observed in mammalian hair cells[37–39]. In the first of these mechanisms, the time course of Ca^{2+} binding to myosin motors and their movement along the actin cytoskeleton is on the order of 10–20 ms, probably too slow to account for the cycle-by-cycle amplification

of stimuli up to 100 kHz seen in some mammals. The characteristic time for Ca^{2+}-dependent channel reclosure in mammalian outer hair cells, however, is in the range of hundreds of microseconds[37], which approaches the speed required for high-frequency amplification.

Integration of motile processes in amplification

Three motile processes operate in the mammalian cochlea: Ca^{2+}-dependent channel reclosure, with a submillisecond time constant; somatic electromotility, with a characteristic time of ~10 ms set by the membrane time constant; and myosin-based adaptation, with a time constant of ~20 ms. What are their roles in amplification? Cycle-by-cycle force generation is most likely mediated by the fastest of these processes, Ca^{2+}-dependent channel reclosure. This mechanism, however, has only a limited dynamic range; its ability to amplify relies on the hair bundle's being poised on the edge of an oscillatory instability characterized by a Hopf bifurcation[18,40,41]. The role of the other two processes could be to position the bundle in such a state so as to maximize the activity of the fast, cycle-by-cycle amplifier[41–43]. Adaptation could act locally on the bundle to adjust the tension in the gating springs, whereas electromotility, with its large dynamic range, might modulate the resonant properties of the cochlear segment in which the hair cell sits. At low frequencies, the receptor potential of the outer hair cell includes an offset potential owing to the asymmetry in the transduction current[44]. In the absence of a cycle-by-cycle signal, this response may provide an error signal for the slower feedback processes, one that could be exploited to set the operating point of the fast amplifier. At high frequencies, however, outer hair cells do not produce such an offset potential[43]. In such cases, stimulation through efferent fibers of the olivocochlear bundle, which has been shown to linearize basilar-membrane responses[45], could act through these slow processes to control amplification. The three motile mechanisms would thus work in concert over a wide range of temporal and spatial scales to provide the ear with a dynamic amplifier.

Methods

In vitro cochlear preparation

Cochleae were excised from 17–28-day-old jirds euthanized with 200 $mg \cdot kg^{-1}$ pentobarbital (Abbott Laboratories, North Chicago, IL) and were placed in dissecting solution containing 145 mM NaCl, 3 mM KCl, 250 μM $CaCl_2$, 250 μM $MgCl_2$, 2 mM sodium pyruvate, 5 mM **D**-glucose, and 10 mM Na_2HPO_4 at pH 7.35. Using a number 11 scalpel blade, we transected the cochlea perpendicular to its main axis between the basal and middle turns and affixed it by the cut bone surface atop a 1.5-mm hole in a plastic disk with cyanoacrylate glue (Iso-Dent, Ellman International, Oceanside, NY). We opened windows in the thin shelves of bone that form the floor and ceiling of the middle cochlear turn, providing a direct optical path through that turn's sensory epithelium. To prevent leakage along the cochlear spiral, all entrances to the cochlear duct were sealed with cyanoacrylate glue. Reissner's membrane was removed and the disk was mounted apical-side-up into a two-compartment recording chamber. This preparation was typically completed in less than 20 min.

The basal surface was bathed in artificial perilymph consisting of dissecting solution with 1.3 mM $CaCl_2$ and 0.9 mM $MgCl_2$; the apical surface was immersed in artificial endolymph comprising 150 mM KCl, 25 μM $CaCl_2$, 1 mM sodium pyruvate, 5 mM **D**-glucose, and 10 mM K_2HPO_4 at pH 7.35. Some experiments used NMDG-based endolymph containing 150 mM NMDG, 25 μM $CaCl_2$, 1 mM sodium pyruvate, 5 mM **D**-glucose, and 10 mM H_3PO_4 at pH 7.35. In others, 1.4 mM amiloride was added to K^+-based endolymph. To ensure complete washout, all solution exchanges were performed twice over 4–5 min. All experimental solutions were oxygenated and used at room temperature. The temperature at the site of the experimental preparation, which was heated by the illumination system, was measured with a copper-constantan thermistor and BAT-8 thermometer (Bailey Instruments, Saddlebrook, NJ).

Animal procedures were performed with approval from the Institutional Animal Care and Use Committee of Rockefeller University.

Acoustic stimulation

Acoustic stimuli were provided by an earphone (ER-1, Etymotic Research, Elk Grove Village, IL) coupled to a port leading to the lower compartment of the recording chamber and driven by a differential amplifier (AM 502, Tektronix, Beaverton, OR) at unity gain. We determined the intensity and frequency profiles of the acoustic pressure stimulus delivered to the cochlear segment by placing a piezoresistive pressure transducer (8507C-1, Endevco, San Juan Capistrano, CA) in place of the preparation and recording the sound pressure in the absence of liquid in the lower compartment. These profiles permitted calibration of the stimuli so that known sound-pressure levels with a flat frequency response from 0.3–3.0 kHz could be delivered to the sensory epithelium. There was a conduction delay of 1.3 ms between the onset of acoustic stimulation and the pressure response at the position of the specimen. All sound-pressure levels are reported with reference to a root-mean-square pressure of 20 μPa. The sound-pressure level (SPL) scale used in this report is a logarithmic representation of the root-mean-square sound pressure relative to this reference value; an increment of 20 decibels (dB) corresponds to an increase in pressure by a factor of ten.

Detection of hair-bundle motion

The displacement of hair bundles of inner hair cells was recorded using procedures analogous to those used to record responses in the bullfrog's sacculus[46]. The hair bundles of inner hair cells were imaged with an upright microscope (MPS, Carl Zeiss, Jena, Germany) fitted with a ×40 water-immersion objective of numerical aperture 0.8 and illuminated with a mercury lamp equipped with a heat filter. The image of the bundle was magnified ×1000 and projected onto a dual photodiode, which permitted detection of sub-nanometer displacements calibrated by imposing a 20-μm offset pulse to the photodiode before each recording. Direct microscopic observation of the organ of Corti confirmed that the hair bundles of inner hair cells were being deflected relative to the reticular lamina.

Laser interferometry

The vertical velocity of the cochlear partition was measured using a Polytec 501 OFV laser interferometer (Polytec, Auburn, MA) coupled into the optical system described above. A 30-μm glass bead was placed on the tectorial membrane above an inner hair cell for signal acquisition. Displacement magnitudes were calculated offline from the interferometric velocity records.

Determination of basilar-membrane stiffness

The passive basilar membrane behaved as a second-order resonant system whose angular resonant frequency ω_0 was determined by its mass m and stiffness K:

$$\omega_0 = \sqrt{\frac{K}{m}}.$$

The mass of the liquid in the upper compartment, which was open to the atmosphere and possessed a wide meniscus, did not affect the resonant frequency and was disregarded in this analysis. We could determine the system's stiffness by varying the mass of the liquid in the lower compartment and measuring the resonant frequency of hair-bundle motion. The mass of perilymph calculated from the length and diameter of the liquid column extending from the sample chamber (m_C) did not include the mass of the dead volume (m_0) directly beneath the basilar membrane. We therefore applied the equation

$$\omega_0^{-2} = \left(\frac{1}{K}\right) m_C + \frac{m_0}{K},$$

in which the slope and intercept of the linear fit of ω_0^{-2} to m_C yielded the stiffness and mass of the dead volume, respectively. To confirm the origin of this measured stiffness in the basilar membrane, we measured the stiffness before and after overnight fixation at 4° in 4% formaldehyde in dissecting solution.

Electrical stimulation and recording

Two pairs of silver-silver chloride electrodes were used to provide electrical currents and measure potentials. Each pair comprised one electrode immersed in the upper-compartment endolymph and a second embedded in agar contacting the lower-compartment perilymph. For electrical stimulation, signals were delivered across the sensory epithelium with a stimulus isolation unit[47] (A395, World Precision Instruments, Sarasota, FL). This unit also provided constant transepithelial currents that reproduced the *in vivo* +80-mV endocochlear potential. Microphonic and transepithelial potentials across the epithelium were monitored by the second pair of electrodes; these signals were amplified ×50,000 before analog-to-digital conversion.

Data collection and analysis

Stimulation and recording were performed using LabVIEW 7.0 (National Instruments, Austin, TX) on a computer (Precision 650, Dell Computer Corporation, Round Rock, TX) at digital output and sampling rates of 20 kHz. All analog input and output signals were subjected to low-pass filtering at 10 kHz with eight-pole Bessel filters.

Data analysis was performed using Excel 2003 (Microsoft Corp., Redmond, WA) and Mathematica 5 (Wolfram Research, Champaign, IL). For determination of hair-bundle displacement at the resonance peak, each frequency spectrum was fit with a Lorentzian curve, from which the peak amplitude was extracted. Linear-regression fits of data points are reported with correlation coefficients; averaged values from repeated experiments are reported as means ± standard deviations. Statistical significance was assessed by Student's one-tailed *t*-test; *P* values less than 0.05 were considered statistically significant.

Acknowledgements

The authors thank A. Hinterwirth for construction of the experimental chamber, B. Fabella for computer programming, and the members of our research group for comments on the manuscript. This work was supported by National Institutes of Health grants DC00241 and GM07739. A.J.H. is an Investigator of Howard Hughes Medical Institute.

References

1. Manley GA. Evidence for an active process and a cochlear amplifier in nonmammals. J Neurophysiol 2001;86:541–9. [PubMed: 11495929]
2. Robles L, Ruggero MA. Mechanics of the mammalian cochlea. Physiol Rev 2001;81:1305–52. [PubMed: 11427697]
3. Ruggero MA, Rich NC, Recio A, Narayan SS, Robles L. Basilar-membrane responses to tones at the base of the chinchilla cochlea. J Acoust Soc Am 1997;101:2151–63. [PubMed: 9104018]
4. Sellick PM, Patuzzi RB, Johnstone BM. Measurement of basilar membrane motion in the guinea pig using the Mössbauer technique. J Acoust Soc Am 1982;72:131–141. [PubMed: 7108035]
5. Overstreet EH, Temchin AN, Ruggero MA. Basilar membrane vibrations near the round window of the gerbil cochlea. J Assoc Res Otolaryngol 2002;3:351–61. [PubMed: 12382108]
6. Ren T, Nuttall AL. Basilar membrane vibration in the basal turn of the sensitive gerbil cochlea. Hear Res 2001;151:48–60. [PubMed: 11124451]
7. Freeman DM, Masaki K, McAllister AR, Wei JL, Weiss TF. Static material properties of the tectorial membrane: a summary. Hear Res 2003;180:11–27. [PubMed: 12782349]

8. Sewell WF. The relation between the endocochlear potential and spontaneous activity in auditory nerve fibres of the cat. J Physiol 1984;347:685–96. [PubMed: 6707972]
9. Ruggero MA, Rich NC. Furosemide alters organ of Corti mechanics: evidence for feedback of outer hair cells upon the basilar membrane. J Neurosci 1991;11:1057–67. [PubMed: 2010805]
10. He DZ, Jia S, Dallos P. Mechanoelectrical transduction of adult outer hair cells studied in a gerbil hemicochlea. Nature 2004;429:766–70. [PubMed: 15201911]
11. Ulfendahl M, Flock Å. In vitro studies of cochlear excitation. Curr Opin Neurobiol 1998;8:475–9. [PubMed: 9751659]
12. Brownell WE, Bader CR, Bertrand D, de Ribaupierre Y. Evoked mechanical responses of isolated cochlear outer hair cells. Science 1985;227:194–6. [PubMed: 3966153]
13. Zheng J, et al. Prestin is the motor protein of cochlear outer hair cells. Nature 2000;405:149–55. [PubMed: 10821263]
14. Santos-Sacchi J. New tunes from Corti's organ: the outer hair cell boogie rules. Curr Opin Neurobiol 2003;13:459–68. [PubMed: 12965294]
15. Liberman MC, et al. Prestin is required for electromotility of the outer hair cell and for the cochlear amplifier. Nature 2002;419:300–4. [PubMed: 12239568]
16. Martin P, Hudspeth AJ. Active hair-bundle movements can amplify a hair cell's response to oscillatory mechanical stimuli. Proc Natl Acad Sci USA 1999;96:14306–11. [PubMed: 10588701]
17. Hudspeth AJ, Choe Y, Mehta AD, Martin P. Putting ion channels to work: mechanoelectrical transduction, adaptation, and amplification by hair cells. Proc Natl Acad Sci USA 2000;97:11765–72. [PubMed: 11050207]
18. Fettiplace R, Ricci AJ, Hackney CM. Clues to the cochlear amplifier from the turtle ear. Trends Neurosci 2001;24:169–75. [PubMed: 11182457]
19. Ricci A. Active hair bundle movements and the cochlear amplifier. J Am Acad Audiol 2003;14:325–38. [PubMed: 14552426]
20. Martin P, Mehta AD, Hudspeth AJ. Negative hair-bundle stiffness betrays a mechanism for mechanical amplification by the hair cell. Proc Natl Acad Sci USA 2000;97:12026–31. [PubMed: 11027302]
21. Choe Y, Magnasco MO, Hudspeth AJ. A model for amplification of hair-bundle motion by cyclical binding of Ca^{2+} to mechanoelectrical-transduction channels. Proc Natl Acad Sci USA 1998;95:15321–6. [PubMed: 9860967]
22. Howard J, Hudspeth AJ. Compliance of the hair bundle associated with gating of mechanoelectrical transduction channels in the bullfrog's saccular hair cell. Neuron 1988;1:189–99. [PubMed: 2483095]
23. Müller M. The cochlear place-frequency map of the adult and developing Mongolian gerbil. Hear Res 1996;94:148–56. [PubMed: 8789820]
24. Hu X, Evans BN, Dallos P. Direct visualization of organ of Corti kinematics in a hemicochlea. J Neurophysiol 1999;82:2798–807. [PubMed: 10561446]
25. Jørgensen F, Ohmori H. Amiloride blocks the mechano-electrical transduction channel of hair cells of the chick. J Physiol 1988;403:577–88. [PubMed: 2473197]
26. Lumpkin EA, Marquis RE, Hudspeth AJ. The selectivity of the hair cell's mechanoelectrical-transduction channel promotes Ca^{2+} flux at low Ca^{2+} concentrations. Proc Natl Acad Sci USA 1997;94:10997–1002. [PubMed: 9380748]
27. Assad JA, Shepherd GM, Corey DP. Tip-link integrity and mechanical transduction in vertebrate hair cells. Neuron 1991;7:985–94. [PubMed: 1764247]
28. Shehata WE, Brownell WE, Dieler R. Effects of salicylate on shape electromotility and membrane characteristics of isolated outer hair cells from guinea pig cochlea. Acta Otolaryngol 1991;111:707–18. [PubMed: 1950533]
29. Corey DP, Hudspeth AJ. Ionic basis of the receptor potential in a vertebrate hair cell. Nature 1979;281:675–7. [PubMed: 45121]
30. Rhode WS, Geisler CD. Model of the displacement between opposing points on the tectorial membrane and reticular lamina. J Acoust Soc Am 1967;42:185–90. [PubMed: 6052076]

31. Naidu RC, Mountain DC. Measurements of the stiffness map challenge a basic tenet of cochlear theories. Hear Res 1998;124:124–31. [PubMed: 9822910]
32. Ohlemiller KK, Siegel JH. The effects of moderate cooling on gross cochlear potentials in the gerbil: basal and apical differences. Hear Res 1992;63:79–89. [PubMed: 1464578]
33. Cooper NP, Rhode WS. Mechanical responses to two-tone distortion products in the apical and basal turns of the mammalian cochlea. J Neurophysiol 1997;78:261–70. [PubMed: 9242278]
34. Cooper NP, Yates GK. Nonlinear input-output functions derived from the responses of guinea-pig cochlear nerve fibres: variations with characteristic frequency. Hear Res 1994;78:221–34. [PubMed: 7982815]
35. Eguíluz VM, Ospeck M, Choe Y, Hudspeth AJ, Magnasco MO. Essential nonlinearities in hearing. Phys Rev Lett 2000;84:5232–5. [PubMed: 10990910]
36. Rybalchenko V, Santos-Sacchi J. Cl^- flux through a non-selective, stretch-sensitive conductance influences the outer hair cell motor of the guinea-pig. J Physiol 2003;547:873–91. [PubMed: 12562920]
37. Kennedy HJ, Evans MG, Crawford AC, Fettiplace R. Fast adaptation of mechanoelectrical transducer channels in mammalian cochlear hair cells. Nat Neurosci 2003;6:832–6. [PubMed: 12872124]
38. Holt JR, Corey DP, Eatock RA. Mechanoelectrical transduction and adaptation in hair cells of the mouse utricle, a low-frequency vestibular organ. J Neurosci 1997;17:8739–48. [PubMed: 9348343]
39. Fettiplace R, Ricci AJ. Adaptation in auditory hair cells. Curr Opin Neurobiol 2003;13:446–51. [PubMed: 12965292]
40. Magnasco MO. A wave traveling over a Hopf instability shapes the cochlear tuning curve. Phys Rev Lett 2003;90:058101. [PubMed: 12633400]
41. Vilfan A, Duke T. Two adaptation processes in auditory hair cells together can provide an active amplifier. Biophys J 2003;85:191–203. [PubMed: 12829475]
42. Kim DO. Active and nonlinear cochlear biomechanics and the role of outer-hair-cell subsystem in the mammalian auditory system. Hear Res 1986;22:105–14. [PubMed: 2426235]
43. Russell IJ, Cody AR, Richardson GP. The responses of inner and outer hair cells in the basal turn of the guinea pig cochlea and in the mouse cochlea grown *in vitro*. Hear Res 1986;22:199–216. [PubMed: 3733540]
44. Dallos P, Santos-Sacchi J, Flock Å. Intracellular recordings from cochlear outer hair cells. Science 1982;218:582–4. [PubMed: 7123260]
45. Murugasu E, Russell IJ. The effect of efferent stimulation on basilar membrane displacement in the basal turn of the guinea pig cochlea. J Neurosci 1996;16:325–32. [PubMed: 8613799]
46. Martin P, Bozovic D, Choe Y, Hudspeth AJ. Spontaneous oscillation by hair bundles of the bullfrog's sacculus. J Neurosci 2003;23:4533–48. [PubMed: 12805294]
47. Bozovic D, Hudspeth AJ. Hair-bundle movements elicited by transepithelial electrical stimulation of hair cells in the sacculus of the bullfrog. Proc Natl Acad Sci USA 2003;100:958–63. [PubMed: 12538849]

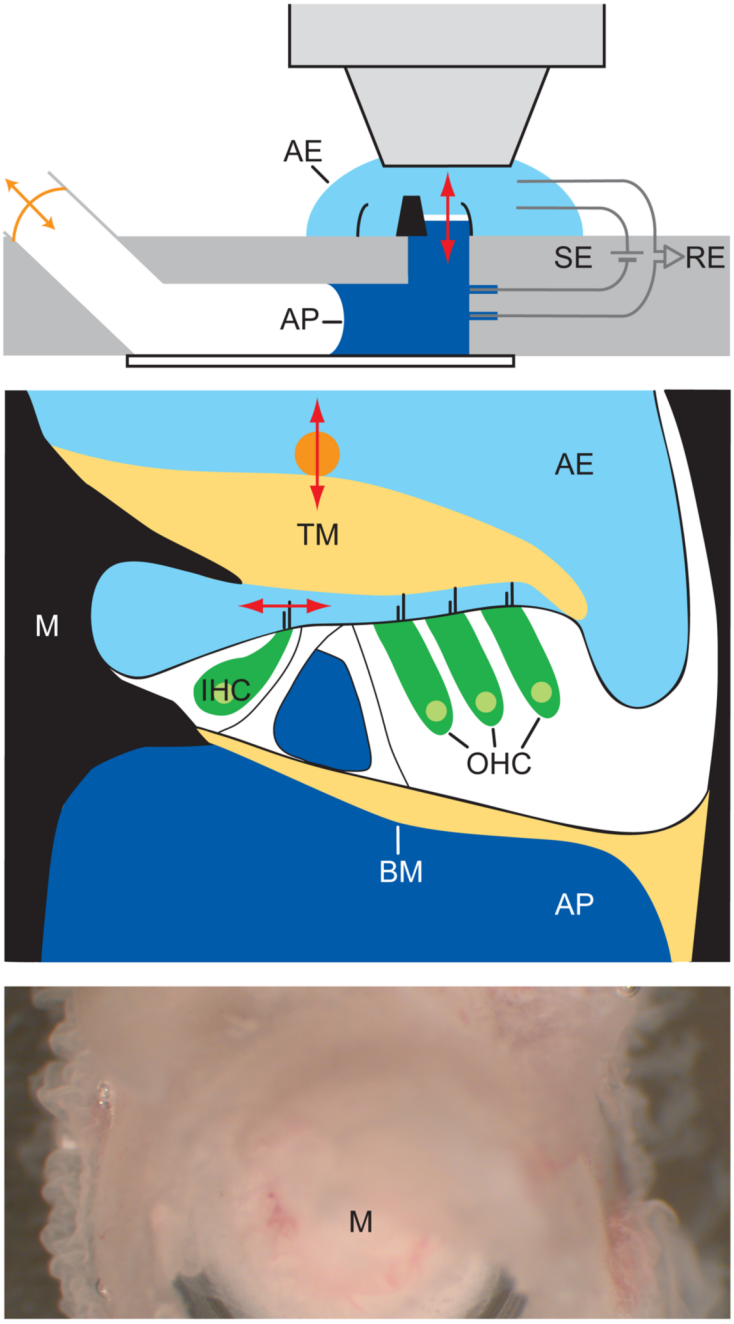

Figure 1.

In vitro cochlear preparation. (**a**) The excised middle cochlear turn, shown in black as transected through the modiolus (center) and outer bony wall, separates the two compartments of the experimental chamber. The apical and basal aspects of the organ of Corti (white) are immersed in artificial endolymph (AE) and artificial perilymph (AP), respectively. Pairs of recording electrodes (RE) and stimulating electrodes (SE) measure microphonic potentials and provide transepithelial electrical stimuli. Acoustic stimuli from an earphone (orange arrow) are delivered to the basilar membrane (red arrow) through the air-and-fluid-filled lower compartment. (**b**) A schematic drawing of the cochlear partition as mounted in the *in vitro* recording chamber shows the organ of Corti (white) suspended between the bone (black) of

the modiolus (M) and outer cochlear wall. The hair bundles of inner (IHC) and outer (OHC) hair cells are stimulated by shearing motions between the basilar membrane (BM) and tectorial membrane (TM). Radial movement of hair bundles of the inner hair cells (horizontal red arrow) is measured with a photodiode; vertical movement (vertical red arrow) was detected with laser interferometry using a glass bead (orange) atop the tectorial membrane. (**c**) A micrograph taken through a dissecting microscope displays the upper surface of the preparation. Three rows of outer hair cells spiral around the cochlear modiolus. (**d**) A video micrograph shows the hair bundles of inner hair cells, one of which is marked (red arrow) to indicate the axis of movements detected with a dual photodiode. (**e**) A similar micrograph shows two of the three rows of outer hair cells and their V-shaped hair bundles. Scale bars: (**c**), 100 μm; (**d**) and (**e**), 10 μm.

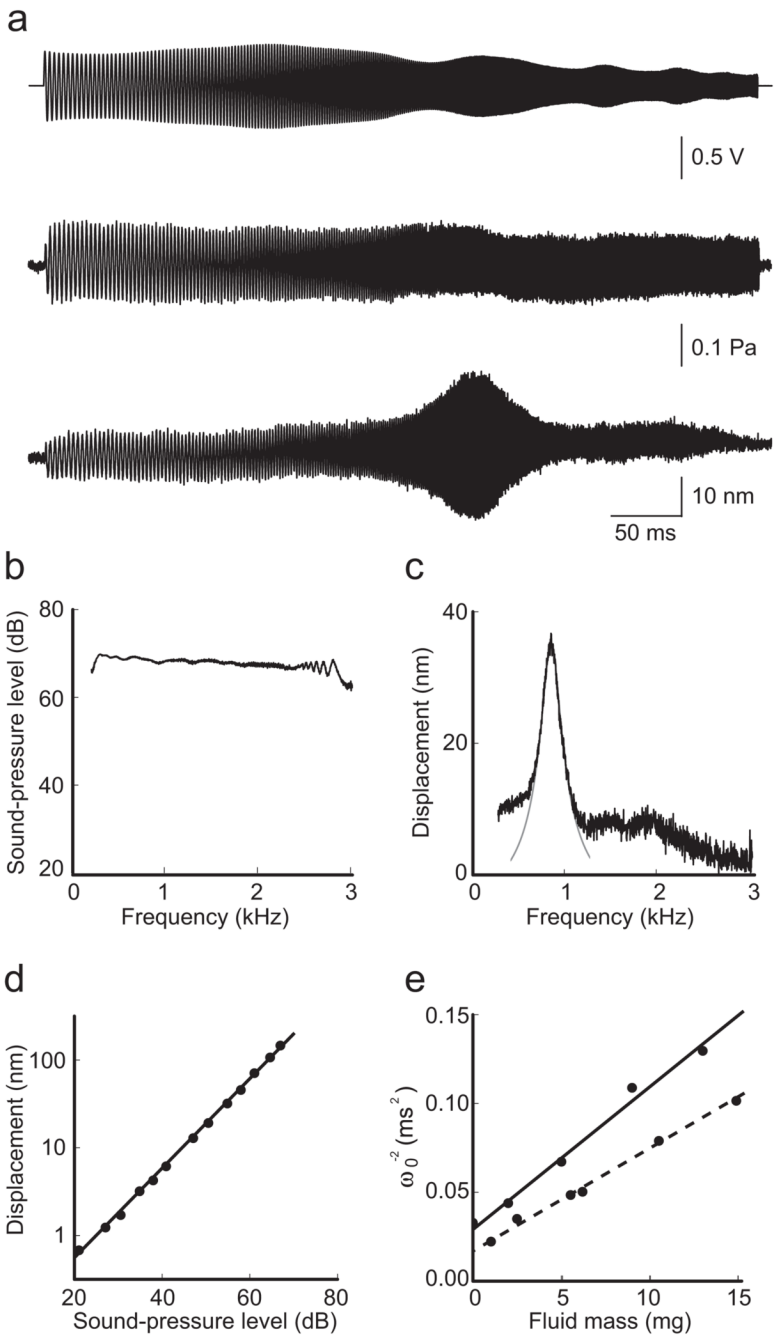

Figure 2.

Basilar-membrane resonance. (**a**) A computer-generated voltage stimulus in the form of a geometric frequency sweep (top) drove an earphone that produced a constant pressure at the basilar membrane (middle) but elicited a striking resonance in the displacement of a hair bundle of an inner hair cell (bottom). (**b**) The frequency spectrum of the applied pressure demonstrates the linearity of the stimulus over the range of frequencies of interest. (**c**) The spectrum of bundle-displacement magnitude reveals a resonance peak at 850 Hz that is well fit by a Lorentzian curve (gray) with a Q_0 of 4.7 and a peak sensitivity of 1.8 μm·Pa^{-1}. (**d**) The response amplitude of a passive hair bundle was linear over a wide range of stimulus intensities. The measured slope in this doubly logarithmic plot (black line) is 1.03 (r^2 = 1.00). (**e**) A plot of the

inverse square of the resonant frequency (ω_0) against the fluid mass in the lower compartment can be fit linearly (solid line) to obtain the stiffness of the system, in this instance 120 $N \cdot m^{-1}$ ($r^2 = 0.98$). Fixation of the same preparation with formaldehyde increased the system's stiffness to 200 $N \cdot m^{-1}$ (dashed line; $r^2 = 0.99$).

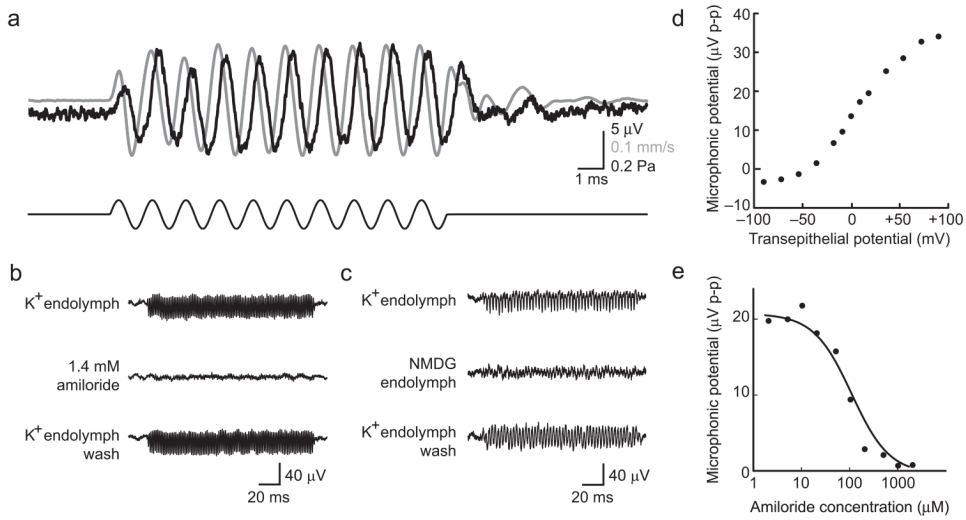

Figure 3.

Microphonic potential. (**a**) Tectorial-membrane velocity (gray) and microphonic potential (black) were recorded simultaneously (top traces) in response to a 67-dB, 800-Hz acoustic stimulus (black, bottom trace) in the presence of a +80-mV transepithelial potential. In this and all subsequent traces, positive polarization of the lower compartment, which correlates with current flowing into hair cells, and vertically upward velocity towards scala media are represented by upward deflections. (**b**) Treatment with amiloride reversibly abolished the microphonic potential in response to sinusoidal stimulation at a resonant frequency of 700 Hz. (**c**) Replacement of the K^+ in endolymph by channel-impermeant NMDG greatly reduced the microphonic response to stimulation at a resonant frequency of 400 Hz. (**d**) The peak-to-peak magnitude of the microphonic potential was dependent on the transepithelial potential, which mimicked the *in vivo* endocochlear potential. (**e**) The concentration-response relationship for amiloride's block of the microphonic potential is fit with a Langmuir isotherm (black line), revealing a K_I value of 96 μM, consistent with the drug's role as a blocker of mechanoelectrical-transduction channels.

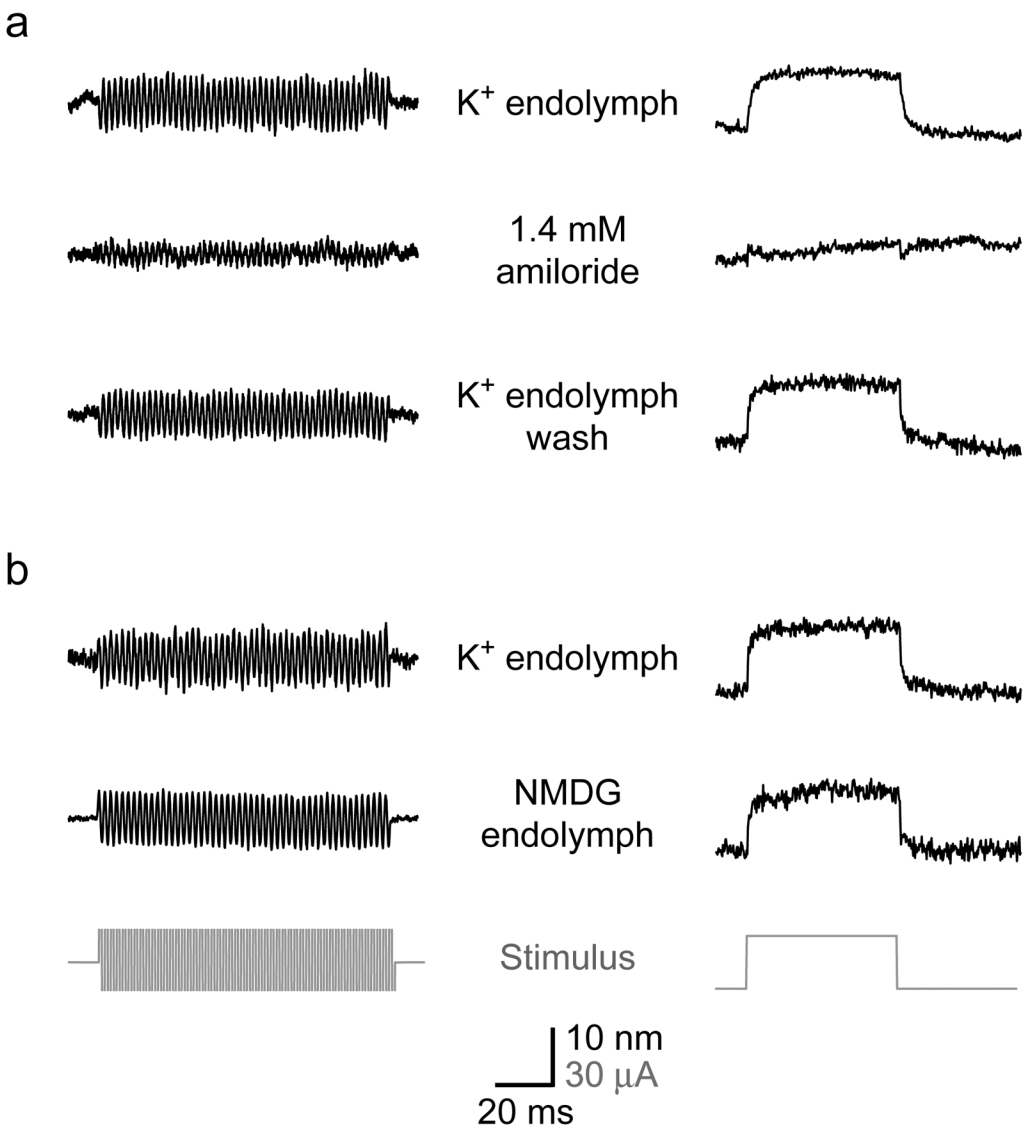

Figure 4.
Electrically evoked hair-bundle movement. The application of sinusoidal (left) or pulsatile (right) current stimuli (gray) across the sensory epithelium evoked hair-bundle movements. (**a**) Treatment with amiloride reversibly diminished both responses, leaving only small transients at transitions in the pulse stimulus. (**b**) In another preparation, substitution of NMDG-based endolymph affected neither the amplitude nor the shape of the responses to electrical stimuli.

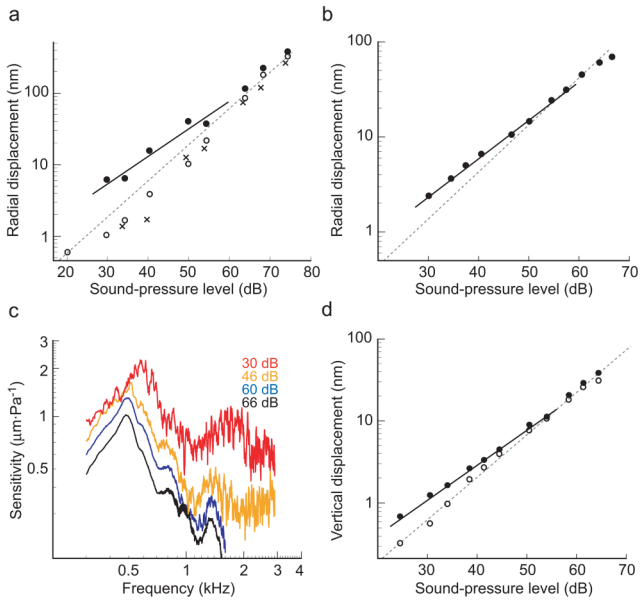

Figure 5.

Compressive nonlinearity and amplification. The amplitude of hair-bundle displacement at the resonance peak was measured over a range of stimulus levels. (**a**) When a +80-mV transepithelial potential was applied in the presence of K^+-based endolymph (closed circles), the power-law slope of the bundle's response (solid line) diverged from linearity (dashed gray line) at low stimulus levels. In contrast, when no transepithelial potential was applied (open circles) or when amiloride was added to the apical solution (crosses), the response became linear. (**b**) When the apical surface was bathed in NMDG-based endolymph, the compressive nonlinearity persisted: the response at low stimulus levels (solid line) diverged from linearity (dashed gray line). (**c**) The nonlinearity is demonstrated in the increasing sensitivity of the response in (**b**) with decreasing sound-pressure level. (**d**) The vertical displacement of the cochlear partition in the presence of a +80-mV transepithelial potential and NMDG-based endolymph (closed circles) also yielded a power-law slope (solid line) that diverged from linearity (dashed gray line) at low stimulus levels. Turning off the transepithelial potential immediately linearized the response in the same preparation (open circles).